Wavelet-based Feature Extraction Algorithm for an Iris Recognition System

Ayra Panganiban*, Noel Linsangan* and Felicito Caluyo*

Abstract—The success of iris recognition depends mainly on two factors: image acquisition and an iris recognition algorithm. In this study, we present a system that considers both factors and focuses on the latter. The proposed algorithm aims to find out the most efficient wavelet family and its coefficients for encoding the iris template of the experiment samples. The algorithm implemented in software performs segmentation, normalization, feature encoding, data storage, and matching. By using the Haar and Biorthogonal wavelet families at various levels feature encoding is performed by decomposing the normalized iris image. The vertical coefficient is encoded into the iris template and is stored in the database. The performance of the system is evaluated by using the number of degrees of freedom, False Reject Rate (FRR), False Accept Rate (FAR), and Equal Error Rate (EER) and the metrics show that the proposed algorithm can be employed for an iris recognition system.

Keywords—Biometrics, Degrees of Freedom, Iris Recognition, Wavelet

1. INTRODUCTION

Irises have approximately 266 distinctive characteristics, of which approximately 173 are used to create the iris template [1]. For this reason, iris recognition is a promising biometric technology. Compared to other biometrics, iris recognition has been around for a shorter period of time. The increasing demand for iris recognition as a security device also demands for the proliferation of its systems, concepts, and algorithms.

The success of iris recognition depends mainly on two factors: image acquisition and the iris recognition algorithm [2]. This study implements a system that considers both factors and focuses on the latter. A central issue with iris pattern recognition is the relationship of inter-class variability and intra-class variability [3]. This is determined by the degrees-of-freedom, which is ideally small for intra-class distribution and large for inter-class distribution. In order to perform successful iris recognition, a representation of images that will create optimal separation among the pattern classes is needed. The standard size of the feature vector used in various studies is 2,048 bits [4, 5], which is not so efficient in terms of storage. Uncompressed image data require considerable storage capacity and transmission bandwidth. Thus, there is a need for better compression algorithms [6]. While there are already existing methods, they have limitations that warrant further study.

This study is a significant endeavor in biometrics that makes use of wavelet transforms in the

Manuscript received February 7, 2011; first revision April 12, 2011; accepted May 16, 2011.
Corresponding Author: Noel B. Linsangan
* School of Electical, Electronics and Computer Engineering, Mapúa Institute of Technology, Manila, Philippines (agpanganiban@live.mapua.edu.ph, {nblinsangan;fscaluyo}@mapua.edu.ph)

 Copyright ⓒ 2011 KIPS (ISSN 1976-913X)

development of iris recognition systems. Furthermore, the results provide information on how to evaluate the accuracy and efficiency of these systems, particularly those that use the wavelet transform as a tool in algorithm development. Hence, this study will serve as a reference for researchers in the field of iris recognition. Moreover, recommendations are given on how to improve the performance of iris recognition systems based on the developed algorithm.

The remainder of this paper is organized as follows. In the next section we present our review of literature on iris recognition and wavelet. The proposed iris recognition algorithm is described in Section 3. In Section 4 we present some experimental results. Finally, conclusions and recommendations are discussed in Section 5.

2. RELATED LITERATURE

A biometric system provides the automatic recognition of an individual based on some unique feature or characteristic possessed by the individual [9]. This section describes the parameters required for iris image acquisition, theoretical background about wavelets, and principles of iris recognition.

2.1 Iris Image Acquisition

In iris image acquisition systems, the average iris diameter is averagely 10 millimeters, and the required pixel number in iris diameter is normally more than 150 pixels. International standards regulate that 200 pixels is of a "good quality," 150-200 is an "acceptable quality," and 100-150 is "marginal quality". Therefore, the iris image with a smaller pixel is considered as being a better quality image and a bigger pixel as being a lesser quality image [10]. Today's camera uses near infrared light to illuminate the subject without causing discomfort.

2.2 Wavelets

Addison [4] describes a wavelet as a mathematical function used to divide a given function or a continuous-time signal into different frequency components and study each component with a resolution that matches its scale. The wavelets are scaled and are the translated copies (known as "daughter wavelets") of a finite-length or fast-decaying oscillating waveform (known as the "mother wavelet"). Wavelet transforms have advantages over traditional Fourier transforms for representing functions that have discontinuities and sharp peaks, and for accurately deconstructing and reconstructing finite, non-periodic, and/or non-stationary signals [5]. These underlying characteristics make wavelets applicable for creating the feature vector that is necessary in the iris recognition algorithm.

2.3 Iris Recognition Algorithms and Principles

Many algorithms have been developed for the iris recognition system. The wavelet functions or wavelet analysis is a recent solution for overcoming the shortcomings in image processing, which is crucial for iris recognition. Nabti and Bouridane proposed a novel segmentation method based on wavelet maxima and a special Gabor filter bank for feature extraction, which obtains an efficient recognition with an accuracy of 99.43% [7]. The steps are as follows: the multi-scale edge detection method is used for iris image processing, the extraction of features

from an iris-polarized image using the proposed Gabor filter bank, and matching with Hamming distance for identification and recognition. Narote et al. proposed a new algorithm for iris recognition based on the Dual Tree Complex Wavelet Transform [8]. The Dual Tree Complex Wavelet Transform (DTCWT) provides three significant advantages: they have reduced shift sensitivity with low redundancy, improved directionality, and explicit phase information. Experimental results show that the above algorithm based on DTCWT is nearly 25 times faster than that of Narote. Also, the authentication using DTCWT demonstrates that the approach is promising in terms of improving iris-based identification.

Masek developed an "open-source" iris recognition system using MATLAB software in order to verify both the uniqueness of the human iris and also its performance [9]. In determining the recognition performance of the system, two databases of digitized grey scale eye images were used. The iris recognition system consists of an automatic segmentation system that is based on the Hough transform, and it is able to localize the circular iris and pupil region, occluding eyelids and eyelashes, and reflections. The extracted iris region was then normalized into a rectangular block with constant dimensions to account for imaging inconsistencies. Finally, the phase data from 1D Log-Gabor filters was extracted and quantized to four levels to encode the unique pattern of the iris into a bit-wise biometric template. The Hamming distance was employed for the classification of iris templates. The system was performed with perfect recognition on a set of 75 eye images. However, tests on another set of 624 images resulted in false accept and false reject rates of 0.005% and 0.238%, respectively [9].

3. PROPOSED METHODS

3.1 Hardware and Software Implementation

The design of the system involves both the hardware and the software to perform iris image capture and iris recognition and these are illustrated in Fig. 1. Using a video camera that captures the texture of the iris image has developed the iris image acquisition system. The camera employs a CCD image sensor. Its focus can be set manually according to user requirements. However, the device alone cannot capture the iris image needed by the proposed software. Lighting and the distance from camera were considered for improving image quality. The lighting source is an infrared light. The diodes give off NIR illumination, which is not visible to the human eye. Since the lighting condition and camera focus may vary for different subjects, an adjustable steel bar support is designed for the camera and the infrared light. By this, the user can set the best distance from the camera and light source by the human eye. If the focus is not properly adjusted, noise can affect the quality of the image. Each iris was sampled once for enrolment and another time for matching. For enrolment, the images were taken after adjusting the focus only once. The same procedure was followed for matching. A chin support was also integrated in the device to adapt to the user. Since the camera used is analog, an analog-to-digital converter is necessary. In this case, a USB DVD Maker is used to integrate the camera to the PC using the composite video input. The image acquisition toolbox of MATLAB connects the camera to a frame grabber in the system computer. The frames are previewed in the customized graphical user interface to allow the user to select among the most appropriate image settings before enrolling it to the iris recognition software.

The Iris Recognition Algorithm block in Fig. 1 illustrates several functions used to determine

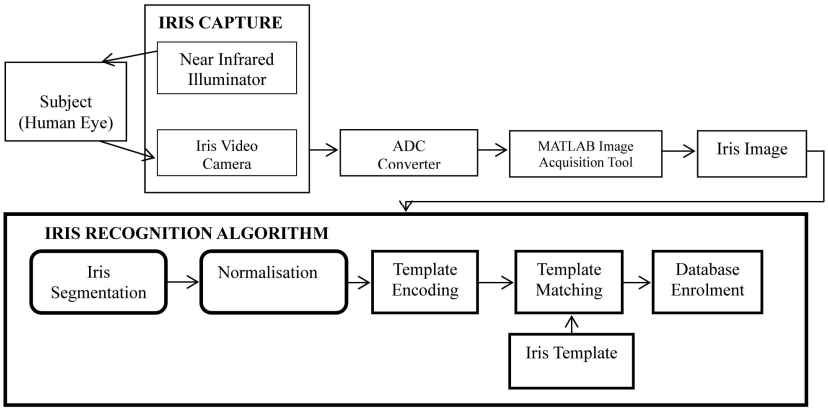

Fig. 1. Iris Recognition System Components

whether an iris image is authenticated. Only the segmentation and normalization processes were based on Masek's method. The rest of the functions, such as feature extraction, were proposed in this study.

In the preprocessing stage, the principle is based on the study of Masek where the image is first converted to an 8-bit grey scale and is reduced to 225 x 300 pixels for faster execution and consistency. The image then undergoes segmentation, normalization, and template encoding. The segmentation process is based on the circular Hough transform, which defines a circle according to the equation,

$$x^2c + y^2c - r^2 = 0. \tag{1}$$

For the captured images, the value of the iris radius ranges from 80 to 150 pixels, while the pupil radius ranges from 20 to 75 pixels. Canny edge detection, a method developed by Canny [11], is employed first to generate an edge map. It uses a multi-stage algorithm to detect a wide range of edges in images. Horizontal lines are drawn for the top and bottom eyelid and two circles are overlaid for iris and pupil boundaries. The process is able to localize the circular iris and pupil region, occluding eyelids and eyelashes, and reflections. Segmentation is highly critical to the success of the iris recognition system. A poor contrast between the iris and pupil and out-of-bound values of iris regions will make segmentation difficult, resulting in poor recognition rates.

In order to allow comparisons, the segmented iris image should undergo the normalization process. This process transforms the extracted iris region into a rectangular block with constant dimensions to account for imaging inconsistencies, which are mainly due to the stretching of the iris from varying levels of illumination. For this study, a radial resolution of 24 pixels and an angular resolution of 240 pixels were used. With these settings, the image can be analyzed using 2D wavelets at a maximum level of 4.

From the normalized region, a biometric template was created. In this study, the wavelet transform was used to extract the discriminating information in an iris pattern. Two mother wavelets namely Haar and Biorthogonal [12] were experimented on. The image was decomposed using the wavelets at N levels where 4 is the maximum. The wavelet transform breaks an

Fig. 2. Wavelet decomposition

image down into four sub-samples or images. The results consist of one image that has been high-pass filtered in the horizontal and vertical directions, one that has been low-pass filtered in the vertical and high-pass filtered in the horizontal, and one that has been low-pass filtered in both directions. Fig 2 illustrates the wavelet decomposition using the MATLAB wavelet toolbox [13].

Looking closely at Fig 2 the patterns of small and large squares were predominantly oriented vertically. With this, vertical coefficient is tested to produce the feature vector. Wavelet coefficients at different levels were also considered to find the best feature vector for the system. Each resulting phase or angle in the complex plane is quantized to the quadrant in which it lies at each local element of the iris pattern. The operation is repeated all across the iris. The binary feature vector is encoded using quantization. Here, coefficients greater than 0.5 are set to a value of 11 while coefficients less than 0.5 are set to 10. The feature vector values falling between 0 to -0.5 are set to 01 and those that are smaller than -0.5 are set to 00.

The encoded bits are stored in a database using the Microsoft SQL Server for template matching. The database columns consist of an auto-incremented iris identification number, iris image path, and iris codes. Table 1 shows the database model.

The last stage of the iris recognition software is the template matching. The matching is employed using the Hamming distance given by the formula,

$$HD = \frac{1}{B}\sum_{i=1}^{B} X_i \otimes Y_i \tag{2}$$

where Xi and Yi represent the i-th bit in the sequences X and Y respectively, and B is the total number of bits in each sequence. The symbol ⊗ is the "XOR" operator. To account for rotational inconsistencies, the template is bit-wise shifted 8 bits to the left and to the right to obtain multiple Hamming distances, and then the lowest distance is chosen.

Fig. 3 illustrates the graphical user interface developed using the MATLAB GUI builder, which contains all the modules for the iris recognition process. The string "Start" shifts to "Stop" and the software starts grabbing frames when the user clicks the start button. The image is captured once the stop button is clicked. If the iris image is for enrollment, the enroll button is

Table 1. Database Structure

Table Name: Iris Data Set		
Column Name	***Data Type***	***Allow Nulls***
IrisImage_id	Int	No
IrisImage_path	varchar (200)	Yes
IrisImage_template	varchar (max)	Yes

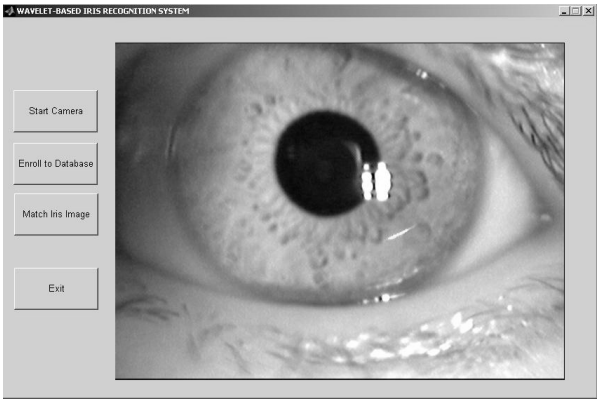

Fig. 3. User interface of the iris recognition software

clicked and the software starts processing the image through the algorithm that was explained earlier. The template is stored in the database with an identification number. If it is for matching, the Hamming distance is calculated to test whether two iris templates are from the same individual or not.

4. RESULTS

The performance of the proposed system was evaluated using the common biometric test metrics to determine whether the objectives of the study were met. The reliability of the algorithm was tested in two modes: verification or the test for inter-class relationship and validation or the test for intra-class relationship. Several iris images were tested from 200 individuals, 100 of which came from the CASIA-IrisV3 collected by the Chinese Academy of Sciences' Institute of Automation (CASIA) [14]. 400 datasets were presented in the study for evaluation. Fig.4 shows the sample datasets. In this figure, ID numbers from 001 to 005 were acquired from the proposed design while ID numbers from 051 to 055 were acquired from CASIA. In the proposed hardware, 2 iris images from the left eye were taken for each individual; one was used for enrollment and the other for template matching. A check on the segmentation result was performed all throughout the trials since segmentation is critical to the success of the iris recognition process. The iris images from different individuals whose templates were first stored in the database were used for matching. Each iris image was encoded as a bit pattern to produce the iris template needed for testing the best wavelet coefficient for the study.

Several testing procedures were employed to evaluate the performance of the proposed algorithm. The first test was employed using two-dimensional discrete stationary wavelet analysis. The decomposition was performed using Haar and Biorthogonal wavelet families at various levels. The vertical coefficient was used as the template encoding parameter and the calculated Hamming distance values for inter-class and intra-class comparisons were tabulated. The minimum and maximum Hamming distance values for inter-class comparisons of templates enrolled in the database were identified. Based on statistics, the number of degrees of freedom is the number of values in the final calculation of statistics that is free to vary [15]. In this context, to test the uniqueness of the iris pattern, the number of degrees of freedom represented by the tem-

ID #	Eye Image	ID #	Eye Image
001	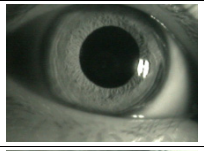	051	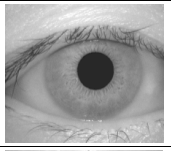
002	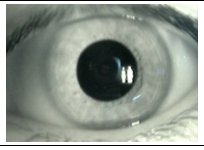	052	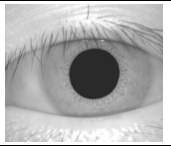
003	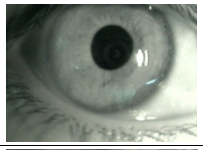	053	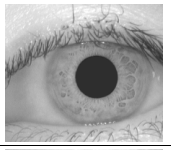
004	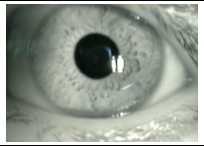	054	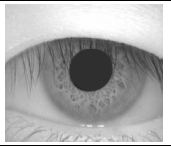
005	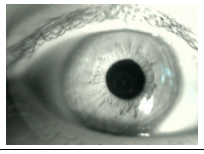	055	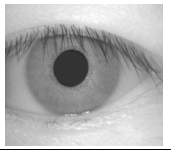

Fig. 4. Iris Images

plates was calculated using the formula,

$$DOF= (\rho(1-\rho))/\sigma^2 \quad , \tag{3}$$

where ρ is the mean, and σ is the standard deviation of the distribution. The collection of inter-class Hamming distance values approximately follows a binomial distribution.

Table 2 shows the summary of results. It can be observed that the template encoded using the Biorthogonal family at Level 1 gives the largest number of degrees of freedom. Hence, it is the most effective in separating the classes.

In order to find out the most efficient wavelet coefficient, the performance of each feature vector was determined in terms of accuracy over vector length or the number of bit patterns.

Table 2. Comparison of the Number of Degrees of Freedom among Different Feature Vectors

Mother Wavelet	*Level*	*Feature Vector*	*DOF*
Haar	1	V	145
Haar	4	V	264
Bior1.3	1	V	280
Bior1.3	4	V	102

Table 3. False Accept Rate and False Reject Rate Values

Mother wavelet	*Level*	*Coefficient*	*FAR*	*FRR*
Haar	1	V	0.07	0.02
Haar	4	V	0.02	0.02
Bior1.3	1	V	0.08	0.07
Bior1.3	4	V	0.08	0.03

Table 4. Comparison of Feature Vector Efficiency Among Different Mother Wavelets

Mother wavelet	Level	Feature Vector	Accuracy in %	Feature vector length
Haar	1	V	93.6	480
Haar	4	V	98.2	120
Bior1.3	1	V	92.5	480
Bior1.3	4	V	94.5	122

Through the range of Hamming distance values, the threshold values were identified. The Equal Error Rate (EER) values were compared amongst the feature vectors. The Hamming distance values were first classified according to three quality classes based on Quality (Q), namely, Poor (P), Moderate (M), and Good (G). Poor Q means that the Hamming distance value is 10 % lower than the threshold value. Moderate Q means that the user has to decide whether the Hamming distance value agrees with the desired result. This occurs when the value is ± 10 % of the threshold values. Good Q means that the Hamming distance value is 10% higher than the threshold value. First, the False Accept Rate (FAR) and the False Reject Rate (FRR) were measured using 100 samples per coefficient. The Hamming distance values that were classified as *M* were excluded in the graph since they do not really provide a concrete decision on template matching. FAR is the probability that the system accepts an unauthorized user or a false template. FRR is the probability that the system rejects an authorized user or a correct template. Table 3 presents the FAR and FRR values. The results show that no perfect recognition is achieved since there is no instance where FRR and FAR values become 0. However, the FAR of 2% and the FRR of 2% for the Haar wavelet decomposed at level 4 give the best results. This suggests that this is the highest in terms of accuracy. This shows that the Equal Error Rate of the system is 2%.

The Correct Recognition Rate (CRR) is the probability that the system will correctly identify the input template from the templates in the database [16]. The CRR of the system was also evaluated over the vector length to test which of the wavelets has the most efficient feature vector. Table 4 shows that the most efficient vector based on the conducted tests is the Haar wavelet decomposed at Level 4, which has a 98.2% CRR for a 120 feature vector length.

5. CONCLUSION

Based on the results, it can be concluded that this study has successfully designed and implemented a wavelet transform based iris recognition system.

The computed number of degrees of freedom based on the mean and standard deviation of the

binomial distribution was able to demonstrate the separation of iris classes. Experimental results show that the Biorthogonal wavelet vertical coefficient at level 4 has the greatest DOF value.

In case a clear decision cannot be made based on a preset threshold value, comparisons between the relative values of Hamming distances can lead to correct recognition. Hence, a conclusive determination of identity can be based on both the threshold value and on a comparison of HD values.

Other biometric test metrics also describe the performance of the system. The FAR and FRR of 2% for Haar wavelet decomposed at level 4 are already acceptable. The results suggest that the Haar wavelet coefficient yields high accuracy and efficiency. The EER of the system is 2%. The Haar wavelet decomposed at Level 4 has a 98.2% CCR for a 120 feature vector length.

It is further suggested that future studies on other mother wavelets be conducted since this study only focuses on Haar and Biorthogonal wavelets. Moreover, the application of wavelet may be expanded in future studies.

REFERENCES

[1] P. Khaw, "Iris Recognition Technology for Improved Authentication", *SANS Security Essentials (GSEC) Practical Assignment*, version 1.3, SANS Institute, 2002, pp.5-8.

[2] A. Basit, M. Y. Javed, M. A. Anjum, *"Efficient Iris Recognition Method for Human Identification"*, World Academy of Science, Engineering and Technology 4, 2005.

[3] J. Daugman, "Demodulation by Complex-Valued Wavelets for Stochastic Pattern Recognition", *International Journal of Wavelets, Multiresolution and Information Processing,* Vol.1, No.1, January, 2003, WSPC/181-IJWMIP 00002, pp.1-17.

[4] S. Lim, K. Lee, O. Byeon, and T. Kim, "Efficient Iris Recognition through Improvement of Feature Vector and Classifier", *ETRI Journal*, Vol.23, No.2, June, 2001.

[5] J. Daugman, "High Confidence Visual Recognition of Persons by a Test of Statistical Independence". *IEEE Transl. on Pattern Analysis and Machine Intelligence*, Vol.15, issue 11, 1993.

[6] T. Yew, *"Detail Preserving Image Compression using Wavelet Transform",* IEEE Region Student Paper Contest UG Category, 1995.

[7] Makram Nabti and Bouridane, "An effective iris recognition system based on wavelet maxima and Gabor filter bank", *IEEE trans. on iris recognition*, 2007.

[8] Narote et al. "An iris recognition based on dual tree complex wavelet transform". *IEEE trans. on iris recognition,* 2007.

[9] L. Masek, *"Recognition of Human Iris Patterns for Biometric Identification",* The University of Western California, 2003.

[10] *Biometric Data Interchange Formats - Part 6: Iris Image Data, Safety of Laser Products - Part 1: Equipment classification Requirements and User's Guide*, IEC 60852-1, 2001.

[11] J. Canny, "A Computational Approach To Edge Detection", *IEEE Trans. Pattern Analysis and Machine Intelligence*, 8:679-714, 1986.

[12] A. Graps, "An Introduction to Wavelets", *IEEE Computational Science and Engineering*, Summer 1995.

[13] M. Misiti, Y. Misiti, G. Oppenheim, and J Poggi, *Wavelet Toolbox 4 User's Guide*, 1997-2009.

[14] CBSR, 2005. Center for biometrics and security research. *CASIA-IrisV3*, http://www.cbsr.ia.ac.cn/IrisDatabase.htm

[15] J. Daugman, "How Iris Recognition Works", *IEEE Proc. on Image Processing,* 2002, doi: 10.1109/ICIP.2002.1037952, pp.33-36.

[16] S. Attarchi, K. Faez, and A. Asghari, *"A Fast and Accurate Iris Recognition Method Using the Complex Inversion Map and 2DPCA"*, *IEEE Conference on Computer and Information Science*, May, 2008, doi:10.1109/ICIS.2008.69, pp.179-184.

Ayra Panganiban

She received her BS and MS degrees in Computer Engineering from Mapúa Institute of Technology in 2010. During 2009-2010, she stayed at Malayan Colleges Laguna, Inc. as Senior Software Engineer and IT lecturer. She is currently a faculty member of the School of Electrical, Electronics, and Communications Engineering at Mapúa Institute of Technology. Her research interests include iris recognition, fuzzy logic, and areas in software engineering, including topics on software reuse, e-learning, and neural networks.

Noel Linsangan

At present, he is the program chair of the Computer Engineering (CpE) program at the Mapua Institute of Technology, Manila, Philippines. Mapua is the largest engineering school in the country. He obtained his baccalaureate degree in Computer Engineering from the same school in 1988 and his Master in Engineering for Computer Engineering from the University of the City of Manila in 2000. Right after graduating from college he joined the faculty of the Computer Engineering program and in 2000 he was appointed as its program chair. His research interests include topics in computer hardware such as digital design, microcontrollers and microprocessors, and computer systems.

Felicito Caluyo

He received his BS in Electrical Engineering and his Master of Engineering from the University of the Philippines Diliman in 1970 and 1977, respectively. He studied in France as a French government scholar and received his Maitrise en Electronique et Communications, Diplome D'etudes Approfondies en Electronique (D.E.A.), and Ph. D in Electronics (Communications Optiques et Microondes) from the Universite de Limoges in 1985, 1986, and 1990, respectively. He was a MERALCO distinguished Professorial Chair on Electronics and Communications engineering at De La Salle University from 1990 up to 2006. He then started at his current post as the Dean of the School of Electrical Engineering, Electronics Engineering, and Computer Engineering at the Mapua Institute of Technology in 2006. His research interests include topics on microelectronics, microwave and optical communications, electromagnetic compatibility, electromagnetic interference, nonlinear circuits and systems, signal processing, control systems and instrumentation, fuzzy systems, neural networks, evolutionary computing, energy systems, solar energy conversion, microhydroelectric power plants, data communications, ATM systems, and management of technology and innovation.